

# Dosimeter arrangement for effective dose and isodose curves determinations into craniofacial cavity

Disposición de dosímetros para determinaciones de curvas de dosis e isodosis efectivas en la cavidad craneofacial

José Daniel Campos Méndez<sup>1</sup>; Gerardo Noguera Vega<sup>1</sup>

---

**CAMPOS, J.D.; NOGUERA, G.** Dosimeter arrangement for effective dose and isodose curves determinations into craniofacial cavity. *J. health med. sci.*, 9(1):45-49, 2023.

**ABSTRACT:** Tomographic dental imaging with cone beam computed tomography has developed so fast in Costa Rica, in the absence of investigations to determine the absorbed dose by the patients, we propose a TLD dosimeter array into RANDO Alderson phantom. Isodose curves were generated by ROOT Data Analysis Framework after an irradiation with Cs-137. The usefulness of the array to measure the dose into the phantom has been proved.

**KEY WORDS:** RANDO Alderson phantom, Isodose curves, Thermoluminescent dosimeter, Cone Beam Computed Tomography.

---

## INTRODUCTION

Because the CBCT images are made by the interaction of the ionizing radiation with the patient, this is absorbing some dose into the process of acquisition. That dose is defined as the energy absorbed by the mass unit, the grey [Gy or J/kg] is the measurement unit use for absorbed dose, however if it is multiplied by a weight factor that depends of the radiation type equivalent dose is obtained, the Sievert [Sv] is the unit used in that case (IAEA, 2007). After a diagnostic acquisition with the CBCT the craniofacial dose values could reach 1073  $\mu\text{Sv}$  (Vano *et al.*, 2015). On the other hand, a dose analysis has been made for different dental CBCT machines and fields of view (FOV), using an anthropomorphic phantom, doses between 69  $\mu\text{Sv}$  and 860  $\mu\text{Sv}$  have been measured (Ludlow, 2009). The need of indicative levels of equivalent dose of tissues and organs in the craniofacial anatomic region, makes of this investigation a beneficial proposal for the Costa Rican population upon the growing of the quantity of dental CBCT machines in the country.

Because the CBCT images are made by the interaction of the ionizing radiation with the patient, this is absorbing some dose into the process of acquisition. That dose is defined as the energy absorbed by

the mass unit, the grey [Gy or J/kg] is the measurement unit use for absorbed dose, however if it is multiplied by a weight factor that depends of the radiation type equivalent dose is obtained, the Sievert [Sv] is the unit used in that case (IAEA). After a diagnostic acquisition with the CBCT the craniofacial dose values could reach 1073  $\mu\text{Sv}$  (Vano *et al.*, 2015). On the other hand, a dose analysis has been made for different dental CBCT machines and fields of view (FOV), using an anthropomorphic phantom, doses between 69  $\mu\text{Sv}$  and 860  $\mu\text{Sv}$  have been measured (Ludlow). The need of indicative levels of equivalent dose of tissues and organs in the craniofacial anatomic region, makes of this investigation a beneficial proposal for the Costa Rican population upon the growing of the quantity of dental CBCT machines in the country.

Any investigation related to dose distribution in the patient of CBCT have been made in Costa Rica by the day that this investigation. Isodose curves maps on the cranio-facial area are necessary to governmental entities as the Health Ministry, to stablish protective barriers to avoid adverse effects of the ionizing radiation and checking the irradiated volume is the same that the image volume.

It is necessary to simulate the dose intake made by the human body. These measurements are

---

<sup>1</sup> Centro de Investigación en Ciencias Atómicas Nucleares y Moleculares, CICANUM, Universidad de Costa Rica.

made using phantoms that represents the different structures and tissues into the human body. Anthropomorphic phantoms simulate the densities into the human body but also simulate the position of the organs and important tissues. The Alderson RANDO is an anthropomorphic phantom with slices 2.5 cm thick, it has spaces to place the dosimeters and its densities are equivalent to the ones in the adult human body (RSD, 2008).

This research looks to create an array made of points into the Alderson RANDO phantom where the TLD crystals could be placed and prove that it works until similar conditions to the ones used in the determination of dental CBCT isodose curves. In this case the phantom will be irradiated with a Cs-137 source.

## MATERIALS AND METHODS

An array was generated where each point has a coordinate (x,y) of its position into the RANDO phantom slice, using the predisposed measurement spaces on it. The points were classified into four quadrants named with the letters A, B, C, D as is seen in the Figure 1. The classification was repeated for all the slices, using the slice thickness the complete head array was created (Figure 2). The coordinates can be associated with the TLD crystal and its later dose value.

Before placing the TLD crystals on the phantom slices, they were cleaned using the cleaning mode in the reader, this machine exposes them to high temperatures to free as many electrons trapped in them as possible, this because the natural radiation interactions. The TLD crystal were places on the respective measurement points but just in half of the spaces, because the plastic support of the dosimeters is much bigger than the sensitive area and the overlap wants to be avoided. The Figure 3 show an example of the setup of one of the slices. 303 TLD crystals were places into the phantom and 12 more were placed in the external surface to the calculation of the skin dose. For each irradiation at least two crystals were taken apart to have the control against natural radiation.

The phantom was irradiated with a Cs-137 source in an anteroposterior position (Figure 4), the

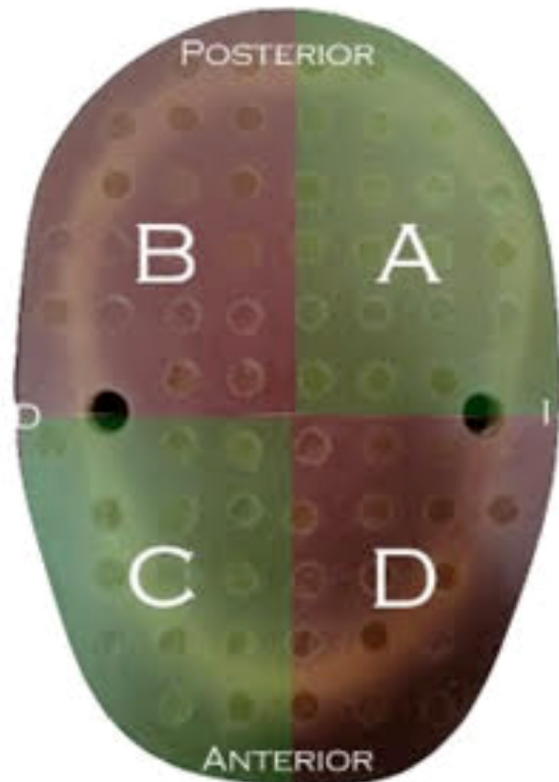


Figure 1. Disposition of the quadrants and the coordinates axis on the RANDO Alderson phantom.

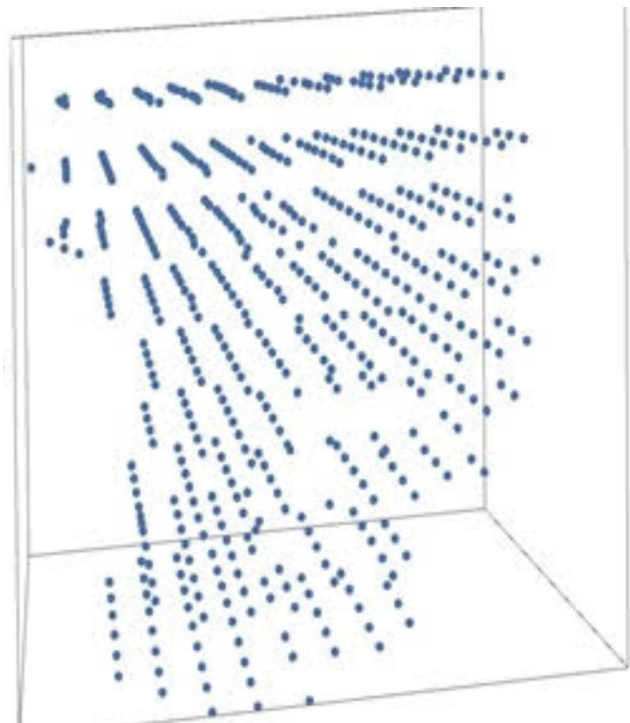


Figure 2. Tridimensional matrix of the available measurement points.



Figure 3. TLD dosimeters placed on one of the slices of the phantom.

source-axis distance was 1 m and the irradiation time were 30 min without any filter between the source and the phantom this is to generate a dose value similar than the one in the dental CBCT acquisition. Because there were not enough dosimeters to fill the complete phantom, multiple irradiations were made under the same conditions, placing the crystal on three slices each time.

The crystals were read, and the data of the measurement was assigned to the specific coordinate on the phantom, the effective dose is found by the multiplication of the generic units of the reading machine to the respective calibration factors. After this calculation the values of the measurement were reported in mSv with an expanded uncertainty of 6.76% with a coverage factor of 2.03 and a confidence of 95.45%. The isodose curves were made for each slice using ROOT Data Analysis Framework (CERN).

## RESULTS AND DISCUSSIONS

After the irradiation the isodose curves were obtained for all the slices of the phantom. Although the dose values cannot be compared with diagnostic acquisitions because a Cs-137 source was used in-

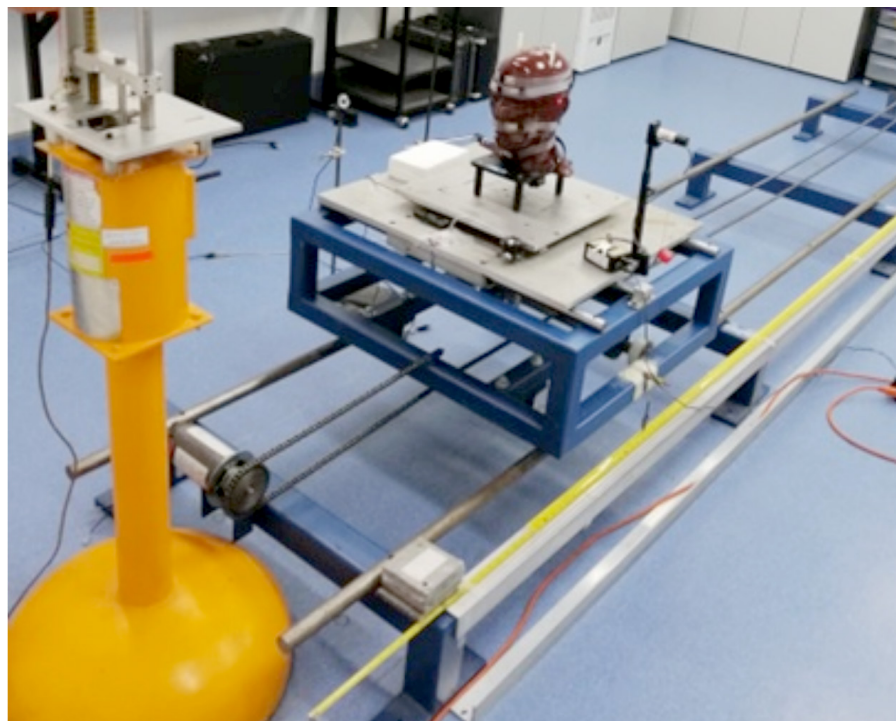


Figure 4. Placement of the phantom in front to the Cs-137 source.

stead a diagnostic X ray tube, the distribution of them should be according to the anatomic characteristics, densities and depth of the different tissues that the phantom is simulating.

The quadrants C and D have higher dose values than A and B. This is an expected result because the last two are posterior so most of the interactions occur near to the entry surface into the C and D quadrants. Another interesting characteristic is the association between the anatomic symmetry with the one represented by the isodose curves; this is an indication that the measurements can be compared with the ones that would be made inside a real patient.

A problem the model could have is because we placed the crystals between the slices and not into them the radiation could reach them without interacting with the phantom going through a too small air gap, something that differs a lot to a real person. However, the problem is not happening, the prove is in the C quadrant slice 1, where the measurement was made in three different points as is shown in the Figure 5. These points are near each other, 1C12 and 1C10 have a similar depth, but the last is into the cranial vault so the dose value is lower than the other two,  $1.110 \pm 0.075$  mSv in 1C14,  $1.030 \pm 0.070$  mSv in 1C12 and  $0.964 \pm 0.065$  mSv in 1C10, this shows the bone attenuation.

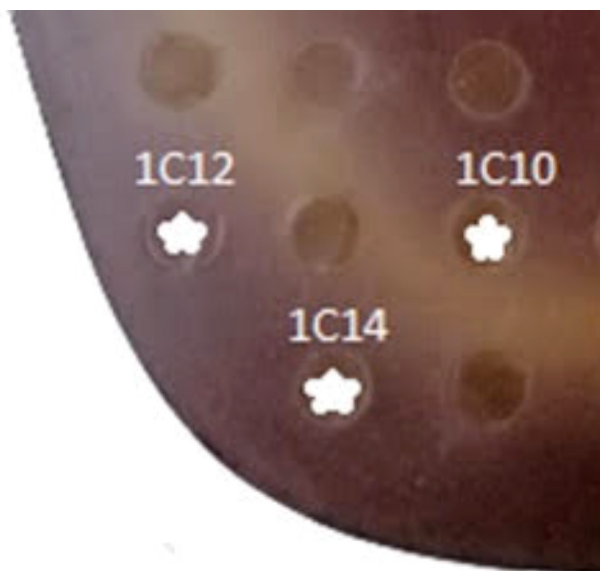


Figure 5. Close up of a section of one slice of the phantom, son measurement coordinates are pointed, the brighter structure represents the bone tissue.

For the skin measurements an average  $1.156 \pm 0.078$  mSv were found, with a standard deviation of 0.069 for the 12 crystals. Higher values at the skin surface are expected because those crystals were irradiated without any extra attenuation and were placed in the frontal side of the phantom. The low standard deviation could be associated to the uniformity of the radiation field of the source.

Isodose curves for each of the nine slices were made by ROOT Data Analysis Framework (CERN, 1996). The Figure 6 shows a decreasing of the dose with the depth from the frontal side, the bendingness of the curves is caused by the natural shape of the face (not flat), the forehead specifically for this slice. With the depth the area for each dose is not linear increasing, this is because the radiation linear attenuation is not linear, a better representation of this behavior could be seen using a homogeneous density phantom.

The RANDO anthropomorphic phantom has a representation of the density of the main structures into the body, placed in the anatomical position. Figure 7 shows a dental CBCT acquisition of the phantom, the different slices and the main bone structures are easy to locate.

The irregularity of the density distribution into the head is increased under the slice 3, because the facial bones, sinuses and soft tissues, this create a more irregular dose distribution compared to slices over 3 (Figure 8).

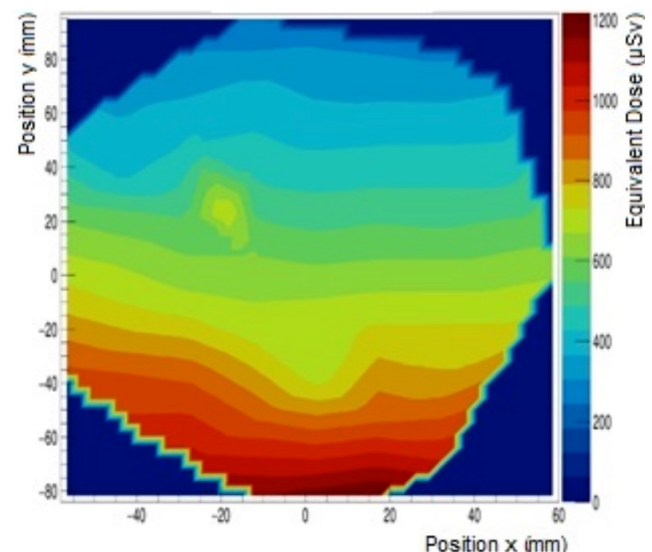


Figure 6. Isodose curves for the slice number two, the color scale, and its reference to  $\mu\text{Sv}$  is showed on the right.



Figure 7. Volumetric reconstruction in of the phantom after a CBCT acquisition. On the bottom, sagittal view of the same acquisition.

The isodose curves can be overlapped on the anatomy of the phantom, Figure 9 shows the isodose curves on the slice 4. The pointed area A show the bent caused by the cranial vault near to the occipital region. B arrow shows how sphenoidal bones makes that the high isodose curves be more superficial because the higher density of the region, also maxilla sinus has a high doses concentration.

The isodose curves do not fit with the phantom contour and they are asymmetric, this is more evident in Figure 8. This is happening because the array of crystals uses the fixed points in the phantom (the darker shadow circles in Figure 9) as a reference to define the position of each dosimeter. Consequently, there are parts of the phantom where dose was not measured. But, in addition to above, only half of the spaces were occupied by a crystal, so there is less information an artifact in the interpolations as the one pointed out by B in the Figure 9, where a possible measuring point is out of the iso-

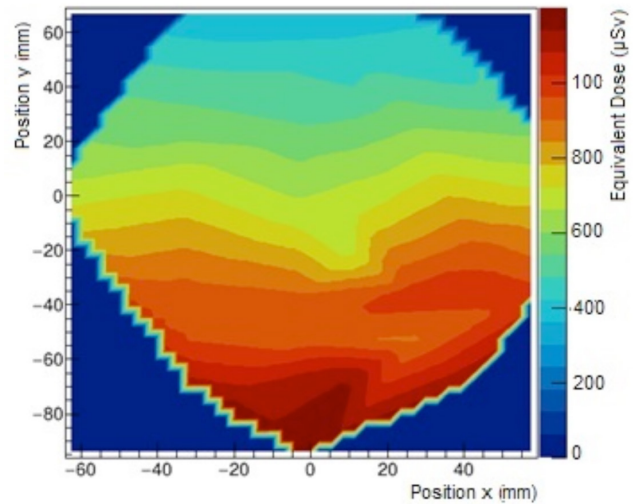


Figure 8. Isodose curves for the slice number four, the color scale, and its reference to  $\mu\text{Sv}$  is showed on the right.

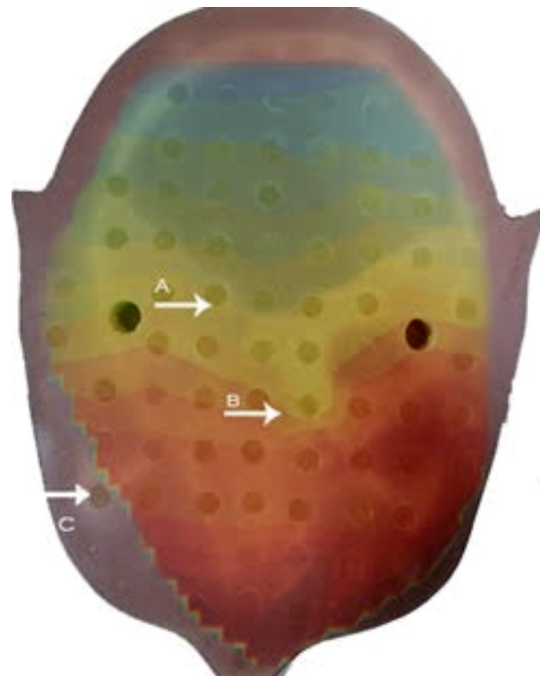


Figure 9. Superposition of the isodose curves on the Figure 7 over the corresponding slice of the phantom. A and B point some deformations, C show a measurement point out of the curves.

dose curves because it was unoccupied and in the outline of the interpolation. These problems could be solved redefining the crystal array, so that it is symmetric, and the phantom contour is included.

Figure 10 shows the dose distribution for slices 3, 5 and 8, the vertical coordinate represents

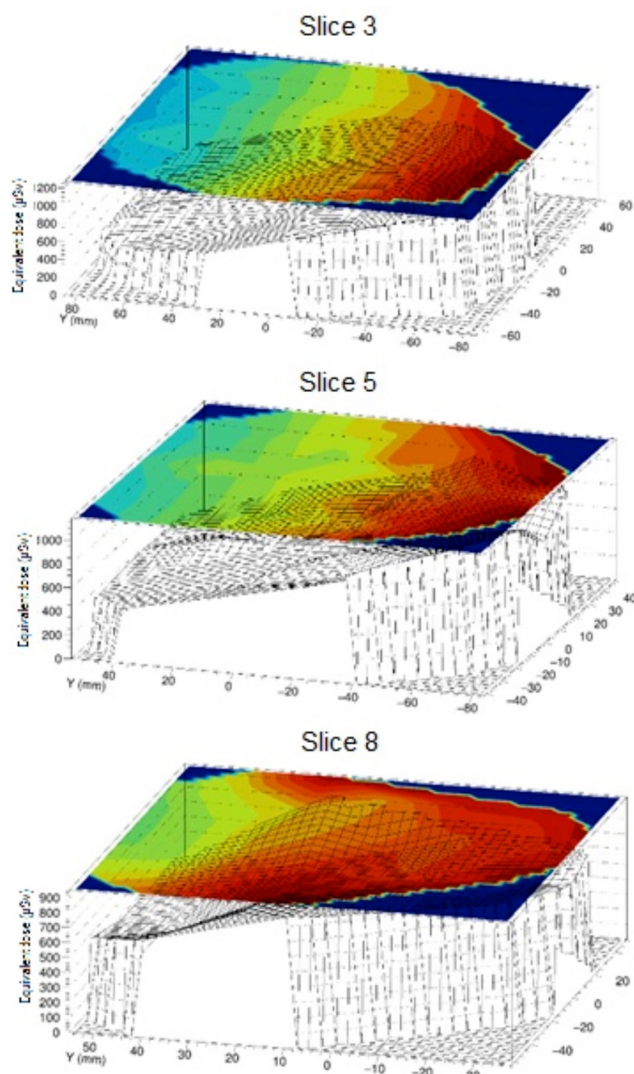


Figure 10. Dose distribution for slices, three (a), five (b), eight (c). The vertical axis represents the dose in  $\mu\text{Sv}$ .

the equivalent dose. This isodose curves seem to match with the anatomy of the phantom, the slice 3 is at the level of the frontal bone, with high density, deeper that is the brain, with low density, that is why the curves are almost symmetric and with an apparently exponential behavior with depth. Differently than above, the slice 5 is at the level of facial bones and paranasal sinuses, so the dose distribution is irregular, in response to the multiple changes of tissue density (bone, water equivalent, air). The high dose curves go deeper in the slice 8, this is according to the anatomy at the level of the neck, higher density structures are in the back (the spine). The isodose curves behavior prove that the array chosen in order to measure the absorbed dose after an irradiation is

appropriate and it could be used for dose determination in dental CBCT irradiations.

## CONCLUSIONS

It is possible to generate a point array into the RANDO Alderson phantom, looking for fixed axis into it, so that all available measurement points have a known coordinate. Measurements must be done in each of the slices, because of the asymmetry of the matrix. It is recommended to find a new method to add more available points, repeatable between measurements and without damaging the phantom.

The proposed array is useful to measurements of the equivalent dose into dental CBCT patients. Isodose curves let know the dose distributions in and between the main organs of the cranial-facial region and part of the neck, also dose can be determined at specific points. To improve this curve, we recommend to include more points into the matrix and placing dosimeters on the skin surface around the phantom, at least each two slices. The superposition of the plastic chips of the dosimeter must be avoided.

## REFERENCES

- CERN. *ROOT Data Analyzer Framework*. 1996, doi:10.5281/zenodo.3895860
- Vano, E.; Miller, D.L.; Martin, C.J.; Rehani, M.M.; Kang, K.; Rosenstein, M.; Ortiz, P.; Mattsson, S.; Padovani, R.; Rogers, A. *Annals of the ICRP*, 129(1), 2015.
- IAEA. "Dosimetry in Diagnostic Radiology: An International Code of Practice". *Technical Reports Series N° 457*, 2007.
- Ludlow, J. "Dose and Risk in Dental Diagnostic Imaging: With Emphasis on Dosimetry of CBCT". *Korean Journal of Oral and Maxillofacial Radiology*, 39(4):175-84, 2009.
- RSD Radiology Support Devices. *The Alderson Radiation Therapy Phantom*. 2008, <https://rsdphantoms.com/radiation-therapy/the-alderson-radiation-therapy-phantom/>

### Autor de correspondencia

Jose Daniel Campos Méndez

Centro de Investigación en Ciencias Atómicas Nucleares y Moleculares, CICANUM,

Universidad de Costa Rica.

E-mail: jose.camposmendez@ucr.ac.cr

Recibido: 15 de Marzo, 2023

Aceptado: 28 de Marzo, 2023